J Solid State Electrochem (2011) 15:2305–2309
DOI 10.1007/s10008-011-1448-y

ORIGINAL PAPER

Diffusion-controlled current at elliptically deformed microelectrodes

Koichi Aoki · Chun Ouyang · Jingyuan Chen · Toyohiko Nishiumi

Received: 30 March 2011 / Accepted: 27 April 2011 / Published online: 18 June 2011

Abstract Diameters of invisible microelectrodes have been estimated from steady-state diffusion-controlled currents of a known concentration of redox species on the assumption of a disk form. However, geometry of the disk is often deformed by polishing the electrode surface obliquely against a polishing pad, by malleability of metal, and/or by distortion of metal wire. Then, the exposed surface is close to an ellipse with rough circumference. The diameter estimated from the steady-state current should be an average value among a major radius, a minor radius, and circumference length. In order to obtain a way of the average, we obtained here voltammetric steady-state currents at elliptic electrodes which were fabricated by polishing glass-coated platinum wire obliquely. Values of the diffusion-controlled currents at the elliptic electrode with smooth edge agreed with the theoretical values with 4% error. The steady-state current at a deformed electrode was approximately proportional to the square root of the area of the electrode rather than the length of the edge, as opposed to the conventional concept of the edge effect on the current. Even if electrode geometry is uncertain, the diameter evaluated from the steady-state current corresponds to the square root of the area.

Keywords Microdisk electrodes · Diffusion-controlled currents · Elliptic electrodes · Geometrical deformation by polishing

K. Aoki (✉) · C. Ouyang · J. Chen · T. Nishiumi
Department of Applied Physics, University of Fukui,
3-9-1 Bunkyo,
Fukui 910-8507, Japan
e-mail: kaoki@u-fukui.ac.jp

Introduction

Microelectrodes have been fabricated either by lithography or polishing inlaid metal wires. The former has advantages of making large amounts of electrodes with ideal geometry. However, it is not suitable to obtain sharp and reproducible current-potential curves owing to difficulty in mechanical polish. In contrast, well-polished inlaid electrodes can provide ideal current–potential curves so far as they are not contaminated. They can take nanometer order in diameter by polishing inlaid wire tips [1–5]. When a metal wire is shielded with glass, the electrode shows higher reproducibility of voltammograms [6–11] than polymer-coated inlaid wires because of tough contact of metal with insulator.

Geometry of the exposed surface of the inlaid electrode is deformed from a disk in the fabrication process, partly because of deviation of the angle between the axis of the wire and the polishing pad from the right angle, partly because of expansion of metal into defective parts at the edge owing to malleability of the metal, and partly because of primordial distortion of the cross section of the wire. Diameters of ultramicroelectrodes have been evaluated from the diffusion-controlled steady-state current at known values of concentration and the diffusion coefficient by use of the theoretical expression for the microdisk electrode, no matter how largely the electrodes may be deformed from a disk. Large deformation at a given electrode area obviously yields a large length of the circumference of the electrode. It is well known that the steady-state current is proportional to the radius of the disk rather than the area because of a predominant contribution of the current density at the edge. Therefore, the deformation would provide overestimation of the radius from the current. This question has frequently been issued when size of invisible electrodes were estimated from their steady-state currents. Unfortunately,

no specific answer has been issued yet, although geometrical effects have been discussed from general viewpoints [12–14].

In order to answer this question, it is necessary to fabricate regularly deformed electrodes. An easy way of the fabrication is to polish inlaid metal wires on a polishing pad at a given angle between the axis of the wire and the pad. Then, the exposed surface becomes an ellipse. If we regard the steady-state current at the elliptic electrode as that of a disk electrode, we get a quantitative relationship between the current and the geometrical deformation. Fortunately, the expression for the steady-state current at an elliptic electrode has been proposed [15] by rewriting the expression for the capacitance of an ellipse in a dielectric medium [16]. Electrode geometry can be evaluated accurately from many coordinate points on the electrode boundary through a microscope [17]. The present paper deals at first with measurements of the steady-state currents at an elliptic electrode in order to confirm the expression for the current. Then, we discuss the significance of radii evaluated from the currents at deformed electrodes.

Experimental

A platinum wire, 0.1, 0.05, or 0.02 mm in nominal diameter, was fixed with a copper alloy wire of conducting lead. A tip of the wire was bent by a given angle (0–75°) and was inserted into a glass tube, as shown in Fig. 1. The tip of the glass was fused with flame of a spirit lamp. It was grinded on emery paper perpendicularly to the axis of the glass until the platinum was exposed. It was polished on a polishing pad with alumina powder and then was washed with water and ultrasonicated in a water bath. When the glass-inlaid wire was polished at a given angle other than the right angle, the electrode did not lie in a same plane. Circumferences were sometimes uneven owing to inclusion of air bubbles in the fuse process and/or expansion of metal into defective parts of glass.

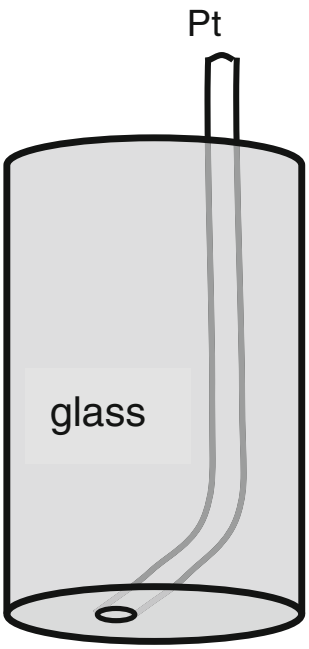

Fig. 1 Illustration of glass-shielded platinum wire

The electrode surface was observed through an optical microscope, VMS-1900 (Scalar, Tokyo) and a scanning electron microscope, S-2600H (SEM, Hitachi). Forty points (x_i, y_i) on the coordinates of the circumference of the electrode were read from the photographs. They were substituted into the general equation of an ellipse, $x_i^2 + Ax_iy_i + By_i^2 + Cx_i + Dy_i + E = 0$. The constants A–E were evaluated by the least square method. The solid curve in Fig. 2 is the fitted curve thus obtained. The general equation was rotated and shifted so that the standard form, $x^2/r_1^2 + y^2/r_2^2 = 1$, was obtained, where r_1 and r_2 are the major radius and the minor radius, respectively.

Acetonitrile solution including 1.12 mM (M=mol dm^{-3}) ferrocene+0.2 M tetrabutylammonium perchlorate (TBA-ClO_4) was prepared. It was deaerated mildly with nitrogen gas. Invariance of concentration change owing to the N_2 bubbling was confirmed by negligible change in voltammetric currents after each bubbling process. Values of the concentration and the diffusion coefficient (D=2.26×10^{-5} cm^2 s^{-1}) were determined from taking the ratio of voltammetric currents at Pt disk electrodes 1.6 and 0.1 mm in diameter [17].

Results and discussion

Voltammograms at the smallest elliptic electrode ($2r_2$= 0.02 mm) are shown in Fig. 3 for two scan rates. Their

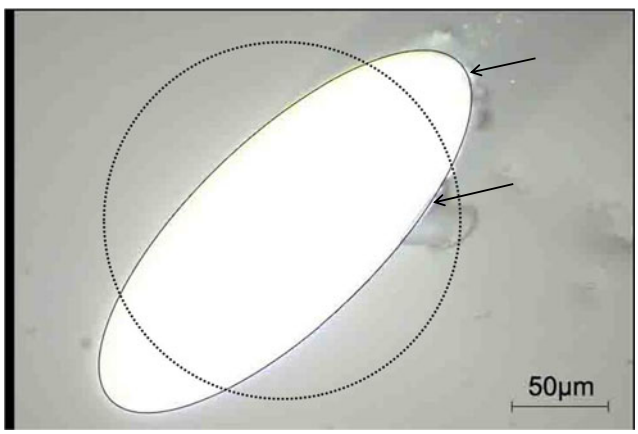

Fig. 2 Photograph of the exposed electrode surface by the optical microscope. The *curve* was calculated from ellipse obtained by the linear least square of 40 points on the peripheral. The *dashed curve* is a circle calculated from the steady-state current at a disk electrode

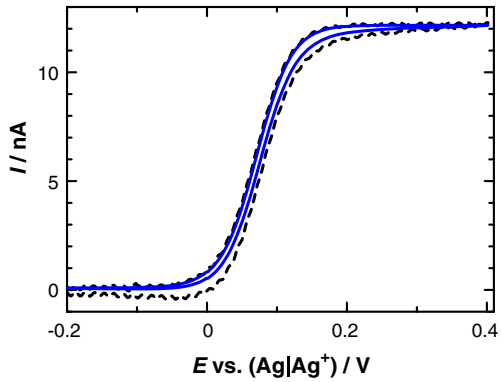

Fig. 3 Voltammograms of 1.12 mM ferrocene+0.2 M $TBAClO_4$ in acetonitrile solution at the electrode (r_1=15.8 μm, r_2=10.3 μm) fabricated by ϕ0.02 mm wire for v=0.01 Vs^{-1} (solid) and 0.05 Vs^{-1} (*dashed*)

limiting currents were independent of the scan rates less than 70 mV s^{-1}. Hysteresis in the voltammograms increased with an increase in the scan rates, probably because of capacitive contribution. A set of coordinate points on the circumference of the electrode was obtained through the optical microscope and the SEM. It was used for the curve fitting of an ellipse and was represented in terms of r_1 and r_2. The two radii were not always determined unequivocally, partly because of unevenness of the circumference, as exemplified in Fig. 2 as the arrowed parts, and partly because of ambiguous focus of the microscope to the circumference. The length of the ambiguity was ca. 1.0 μm. Values of the radii are listed in Table 1.

The steady-state current at an elliptic electrode has been predicted from the derivation of capacitance of an elliptic plate in a uniform dielectric medium [16]. The current for a one-electron transfer reaction is expressed by [15]

$$I_{\mathrm{E,ss}} = 2\pi Fc^{*}Dr_1/K\left(\sqrt{m}\right) \tag{1}$$

where $K(m)$ is the complete elliptical integral of the first kind [18] and m is the eccentricity of the ellipse, defined by $m^2=1-(r_2/r_1)^2$. Here, c^* and D are concentration and the diffusion coefficient of the redox species, respectively. Values of $I_{\mathrm{E,ss}}$ were calculated from known values of c^*, r_1, r_2, and D by inserting them into Eq. 1, where numerical values of K were computed by the approximate equation [18]. Relative errors of experimental value of $I_{\mathrm{E,ss}}$ from Eq. 1, listed in Table 1, are within 4% at electrodes for nominal $2r_2$=0.02 mm. These small errors should be accidental because measurements of the diameters included ambiguity of 1 μm. Larger electrodes should have smaller errors.

Large electrodes ($2r_2$=0.1 mm), of which geometry can be evaluated accurately, have a problem exhibiting unsteady-state voltammogram even at practically slow scans, as shown in Fig. 4. Hysteresis of the voltammograms still remained at v=10 mV s^{-1}. The voltammetric diffusion-controlled peak current at the disk electrode r_0 in radius is expressed for any scan rate by [17, 19]

$$\begin{aligned} I_{\mathrm{D}} &= I_{\mathrm{D,ss}}\left(0.34\mathrm{e}^{-0.66p} + 0.66 - 0.13\mathrm{e}^{-11/p} + 0.352p\right) \\ &\approx I_{\mathrm{D,ss}}\left(1 + 0.128 \quad r_0\sqrt{vF/RTD}\right) \end{aligned} \tag{2}$$

where $I_{\mathrm{D,ss}}=4Fc^{*}Dr_0$ is the steady-state current, and $p=r_0(vF/RTD)^{1/2}$. The current for small values of p, given on the right hand side of Eq. 2, should vary linearly with $v^{1/2}$. We applied this linear relation to the peak currents, I_{E}, at elliptic electrodes with $2r_2$=0.1 mm in order to obtain the steady-state current, as shown in Fig. 5. The current values fell on a straight line, the intercept of which should provide the steady-state current. The currents calculated from Eq. 1 are depicted with dashed lines in Fig. 5. The intercept values for $r_2/r_1\geq$0.57 (c–f) agreed with the theoretical ones within the error of 3%, whereas those for $r_2/r_1\leq$0.38 (a, b) were larger than the theoretical ones. The voltammetric behavior at an elliptic electrode at $r_2<<r_1$ is predicted to be closer to that at a band electrode rather than at a disk electrode. Then, the peak current gets inversely proportional to $\ln(2RTD/Fr_1^2v)+3$ [20]. It tends to zero for $v\rightarrow 0$. The forced extrapolation of I_{E} to v=0 for $r_2<<r_1$ must cause overestimation of the steady-state current, as is consistent with the difference between the intercept and the dashed line. Slopes of the solid lines in Fig. 5 increased with a decrease in r_2/r_1 or a decrease in r_1 for a given value of r_2. The increase in the slopes means a large deviation from the steady state.

It is interesting to compare r_1 or r_2 with the radius which is evaluated from the diffusion-controlled steady-state

Table 1 Electrode geometry and steady-state currents

	r_1/μm	r_2/μm	Nominal r/μm	$I_{\mathrm{E,ss}}$/nA	$(I_{\mathrm{E,ss}})_{\mathrm{exp}}/(I_{\mathrm{E,ss}})_{\mathrm{theory}}$	$I_{\mathrm{def,ss}}/(I_{\mathrm{E,ss}})_{\mathrm{exp}}$
1	15.8	10.3	10	11.0	0.98	1.13
2	13.3	10.5	10	10.7	1.04	1.07
3	55.1	54.1	50	51.4	1.01	1.04
4	66.5	53.3	50	62.7	0.98	0.93
5	73.5	53.1	50	56.3	1.03	1.08
6	99.2	51.9	50	73.5	0.99	0.95

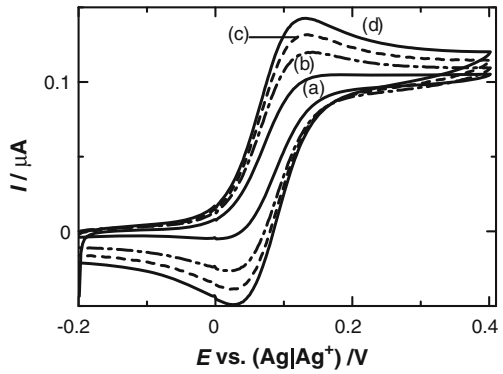

Fig. 4 Voltammograms of 1.12 mM ferrocene+0.2 M $TBAClO_4$ in acetonitrile solution at the electrode (r_1=81.5 μm, r_2=28.6 μm) fabricated by ϕ0.1 mm wire for v=0.01 Vs^{-1} (**a**), 0.03 Vs^{-1} (**b**), 0.05 Vs^{-1} (**c**), and 0.07 Vs^{-1} (**d**)

current on the assumption of a disk. This discussion corresponds to estimating the averaged radius, $r_{0,av}$, from $I_{E,ss}$ through the equation

$$I_{E,ss} = 2\pi Fc^* D r_1 / K\left(\sqrt{m}\right) = 4Fc^* D r_{0,av} \tag{3}$$

Values of $r_{0,av}$ should vary with r_2/r_1 and r_1. They were normalized with the length of the circumference of the ellipse on the prediction that the current density is extremely high at the edge of the electrode, like at a disk electrode. The length of the circumference is given approximately by [21]

$$L \approx \pi(r_1 + r_2)\left[1 + 3\left(\frac{r_1 - r_2}{r_1 + r_2}\right)^2 \Big/ \left(10 + \sqrt{4 - 3\left(\frac{r_1 - r_2}{r_1 + r_2}\right)^2}\right)\right] \tag{4}$$

Figure 6 shows the variation of $2\pi r_{0,av}/L$ with r_2/r_1. Values of $2\pi r_{0,av}/L$ decrease more largely as r_2 is smaller than r_1. This disappointment implies that the infinite current density at the edge does not highly contribute to the total current. This implication can be supported by the following calculation. The current density at radius r on the disk electrode is proportional to $(r_0^2 - r^2)^{-1/2}$ [22]. The partial current on the ring from a radius at qr_0 ($0<q<1$) to the edge, which is normalized by the total current, is given by

$$I_q / I_{q=1} = \int_{qr_0}^{r_0} \left(r_0^2 - r^2\right)^{-1/2} \mathrm{d}r \Big/ \int_0^{r_0} \left(r_0^2 - r^2\right)^{-1/2} \mathrm{d}r = (2/\pi)\sin^{-1} q \tag{5}$$

Values for q=0.8 and 0.9 are 0.59 and 0.71, respectively. Therefore, the large current density near the edge is not a principal role of the total current.

We failed to express approximately the current as the length of the circumference. We attempt to normalize the average radius with the geometric mean of r_1 and r_2, which is proportional to the square root of the area ($\pi r_1 r_2$) of the ellipse. Figure 6 also shows the variation of $r_{0,av}/(r_1 r_2)^{1/2}$ with r_2/r_1. A slight change in r_2 from r_1 decreases largely $r_{0,av}$. No matter largely deviates the disk, values of $r_{0,av}/(r_1 r_2)^{1/2}$ are within $0.9(r_1 r_2)^{1/2}$. This result has been theoretically inferred for microelectrodes of arbitrary shape [23]. In other words, the steady-state current at a deformed electrode with the area S can be approximated as

$$I_{def,ss} \approx 4Fc^* D\sqrt{S/\pi} \tag{6}$$

Let $(I_{E,ss})_{exp}$ be the steady-state current experimentally obtained. Relative errors, $I_{def,ss}/(I_{E,ss})_{exp}$, calculated from Eq. 6 are listed in Table 1. The errors are ca. 10%. The approximation of Eq. 6 is a new insight into estimating currents at deformed electrodes.

Now, we consider dependence of the current on the average radius of the electrode which is polished with the angle θ between the axis of the cylindrical wire electrode and a polishing pad. Because of $r_2/r_1=\sin\theta$, we can determine values of $r_{0,av}/(r_1 r_2)^{1/2}$ from the curve in Fig. 6. It is possible to polish the wire at $\theta=(90\pm15)°$. Consequently, we can fabricate electrodes which fulfill $0.95<r_{0,av}/(r_1 r_2)^{1/2}<1$.

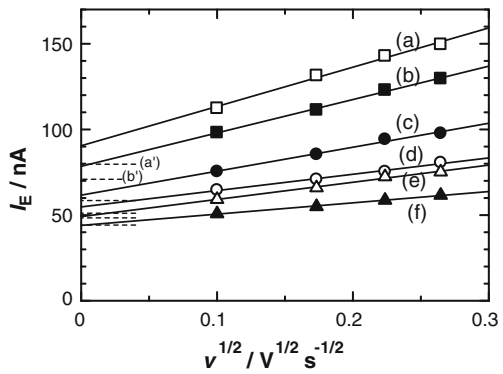

Fig. 5 Dependence of the limiting or the peak currents at the electrodes with geometry of r_2/r_1=0.35 (**a**), 0.40 (**b**), 0.27 (**c**), 0.72 (**d**), 0.80 (**e**), and 0.98 (**f**) on square roots of the scan rates. *Dashed lines* denote theoretical values calculated from Eq. 2

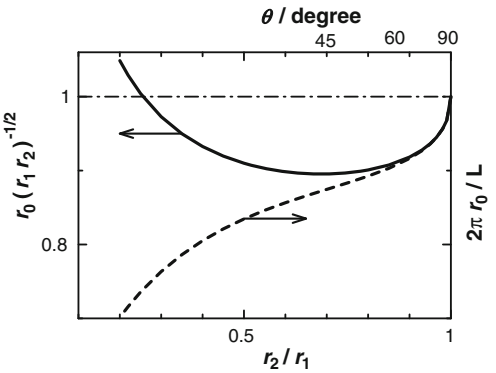

Fig. 6 Variations of $r_0(r_2 r_1)^{-1/2}$ and $2\pi r_0/L$ with r_2/r_1, calculated from Eqs. 3 and 4

Conclusion

The diffusion-controlled steady-state currents at elliptic electrodes obey Eq. 1 for $0.35<r_2/r_1<0.98$ experimentally. Although ideal elliptic form can be fabricated for larger electrodes, largely deformed electrodes for $2r_2=0.1$ mm hardly show steady-state voltammograms.

The steady-state current at a deformed electrode is approximately proportional to the square root of the area of the electrode rather than the length of the edge. When we evaluate a radius of an invisible disk-like electrode from the steady-state current, the radius means any geometry with the area of πr_{av}^2.

Acknowledgments This work was financially supported by Grants-in-Aid for Scientific Research (grants 22550072) from the Ministry of Education in Japan.

References

1. Conyers JL Jr, White HS (2000) Anal Chem 72:4441–4446
2. Menon VP, Martin CR (1995) Anal Chem 67:1920–1928
3. Penner RM, Heben MJ, Longin TL, Lewis NS (1990) Science 250:1118–1121
4. Mirkin MV, Richards TC, Bard AJ (1993) J Phys Chem 97:7672–7677
5. Chen J, Aoki K (2002) Electrochem Commn 4:24–29
6. Pendley BD, Abruna HD (1990) Anal Chem 62:782–784
7. Zoski CG, Liu B, Bard AJ (2004) Anal Chem 76:3646–3654
8. Lee C, Miller CJ, Bard AJ (1991) Anal Chem 63:78–83
9. Wang G, Bohaty AK, Zharov I, White HS (2006) J Am Chem Soc 128:13553–13558
10. Aoki K, Zhang C, Chen J, Nishiumi T (2010) Electrochim Acta 55:7328–7333
11. Li Y, Cox JT, Zhang B (2010) J Am Chem Soc 132:3047–3054
12. Senthamarai R, Rajendran L (2008) Electrochim Acta 53:3566–3578
13. Aoki K (1993) Electroanalysis 5:627–639
14. Zhu H, Tolmachev YV, Scherson DA (2010) J Phys Chem C 114:13650–13656
15. Bruckenstein S, Janiszewska J (2002) J Electroanal Chem 538:3–12
16. Smythe WR, Yeh C, Grey DE (1972) Electricity and magnetism. In: American Institute of Physics handbook, 3rd edn. McGraw Hill, New York
17. Zhang H, Aoki K, Chen J, Nishiumi T, Toda H, Torita E (2011) Electroanalysis 23:947–952
18. Abramowitz M, Stegun I (1964) Handbook of mathematical functions. Dover, New York, pp 589–591
19. Aoki K, Akimoto K, Tokuda K, Matsuda H, Osteryoung J (1984) J Electroanal Chem 171:219–230
20. Aoki K, Tasakorn P, Chen J (2003) J Electroanal Chem 542:51–60
21. Wikipedia. Ellipse. http://en.wikipedia.org/wiki/Ellipse. Accessed 21 March 2011
22. Newman JS (1973) Electrochemical systems. Prentice-Hall, Upper Saddle River, p 344
23. Oldham KB (1992) J Electroanal Chem 323:53–76